Wavepacket scattering from an attractive well

2001 J. Phys. A: Math. Gen. 34 3841

(http://iopscience.iop.org/0305-4470/34/18/312)

INSTITUTE OF PHYSICS PUBLISHING JOURNAL OF PHYSICS A: MATHEMATICAL AND GENERAL

J. Phys. A: Math. Gen. **34** (2001) 3841–3857 www.iop.org/Journals/ja PII: S0305-4470(01)15836-1

Wavepacket scattering from an attractive well

G Kälbermann

Soil and Water Department, Faculty of Agriculture, Hebrew University, Rehovot 76100, Israel

E-mail: hope@vms.huji.ac.il

Received 24 July 2000, in final form 27 February 2001

Abstract

Wavepacket scattering off an attractive well is investigated in two spatial dimensions numerically. The results confirm what was found previously for the one-dimensional case. The wave scattered at large angles is a polychotomous (multiple-peak) coherent train. Large-angle scattering is extremely important for low impinging velocities and at all impact parameters. The effect disappears for packets more extended than the well. Experiments to detect the polychotomous behaviour are suggested.

PACS number: 0365N

1. Introduction

One-dimensional wavepacket scattering off an attractive potential well was investigated in a previous work [1]. In spite of being a thoroughly studied example of quantum scattering for plane-wave stationary states, the effect found for packets, was unknown at that time.

Packets that are narrower than the well width initially, recede from the well in the form of a multiple-peaked wave train. Packets that are wider than the well, do not show this behaviour. A smooth wave hump proceeds both forwards and backwards. Moreover, for narrow packets, the reflected waves dominate and scatter back from the interaction region with an average speed that is independent of the initial average speed of the packet, whereas the transmitted waves proceed in accordance with expectation.

Although wavepackets seem to occupy a place of honour in the educational literature of quantum mechanics [2], they are virtually absent from the research literature. Only fairly recently, and mainly due to the arrival of Bose trap methods, there has been a resurgence of interest in the subject [3]. Conventional scattering processes are dealt with by using plane waves for the incoming flux of particles. The justification for the approach, stems from the fact that, accelerators generate beams of particles that are almost monochromatic in energy (momentum), and extremely spread in spatial extent [4]. For such beams, the packets look more like a plane wave, and, may be treated theoretically using stationary states.

The size of packets in actual scattering reactions is in any case enormous compared with the size of scatterers, therefore, the dependence on packet details is irrelevant.

0305-4470/01/183841+17$30.00

Some exceptions apply, however, for atomic scattering processes, such as those investigated in chemical physics [5]. The semiclassical approximation is used in the study of those processes to describe the actual motion of individual atoms.

Present-day capabilities of accelerators impede the production of particle beams of spatial extent smaller than the size of the scattering agents. Even optical pulses in the femtosecond range are still wider than the size of atoms from which they scatter. It is, nevertheless, not totally unrealistic to expect that the situation may change in the near future. The import of the present paper reinforces the need to produce narrow packets and design suitable experiments.

The technique of cold Bose traps may serve as such a set-up, because of the relative ease in handling beams of atoms at low energy and their subsequent scattering inside cavities taking the role of potentials. In such an experiment with a narrow bunch of atoms, the scattered atoms will proceed in a manner resembling the coherent light emerging from a laser.

The *ALAS* phenomenon in nuclear physics [6] may also be related to the present findings, as described in section 4.

Polychotomous (multiple-peak) waves are observed when a superintense laser field focuses on an atom [7]. Ionization is hindered and the wavefunction is localized, in spite of the presence of the strong radiation field.

In section 2 we will summarize and expand the results of the previous work on the one-dimensional case. Section 3 will describe two-dimensional scattering. Some experiments are proposed in section 4.

2. One-dimensional packet scattering off an attractive well

In a previous work [1], it was found that, a multiple-peak coherent wave train is reflected from an attractive well, when the incoming packet is narrower than the well. These waves spend a large amount of time spreading out of the scattering region. The average speed of the reflected wave was found to be independent of the average energy of the packet.

The scattering was investigated within the framework of non-relativistic potential scattering. Narrow wavepackets have high-frequency modes. One could suspect the approach not to be consistent, due to the emergence of relativistic corrections for these modes. However, we took precautions by choosing a very large mass as compared with the inverse of the packet spread. We took $m = 20$, while the width of the packet was $\Delta x^{-1} \approx 2$ at least. For such a large mass, the speed of propagation of the frequency modes at the edge of the spectrum of the packet is still small in value, less than $v = 1$ in our units.

Moreover, as will be depicted below, we are looking at an effect that unfolds immediately after the packets start to swell and not at very long times for which one could doubt the validity of a non-relativistic approach. The multiple-peak behaviour appears at times shorter than the spreading time of the packet. The relativistic corrections are then expected to be of a lesser concern.

A correct treatment of high frequencies or high momenta demands a relativistic wave equation. Other wave equations must be considered in order to assess the correctness of the above assumptions, such as the Klein–Gordon equation or the Dirac equation. In spite of the limitations of the Galilean invariant Schrödinger equation, it has proven quite successful in atomic, molecular and nuclear processes, even for time-dependent reactions, as that dealt with presently. This is the reason we opted for the non-relativistic potential scattering approach.

A narrow packet scatters backwards as a polychotomous wave train, that is generated from the interference between the incoming wave and the reflected wave. For a narrow packet, the interference pattern is not blotted out as time passes. A very broad packet resembles more a plane wave, its spread in momenta is much smaller than that of a narrow packet.

When the well reflects waves in the backward direction, they interfere destructively with the incoming broad packet, erasing the polychotomous behaviour. A thin packet having short-wavelength components of the order of the well width (slit) produces a cleaner diffraction pattern. Constructive interference with the incoming packet allows the pattern to survive.

Quantum mechanics textbooks show pictures of the development of wavepacket scattering from wells and barriers [8]. Large oscillations of the wavefunction are seen when a packet is traversing a well. These oscillations are propagated only in the backward direction.

Only wide packets, as compared with the width of the well, are shown in the literature. The effect of the width of the packet is not investigated. What was found in [1] and extended here, is that the oscillatory behaviour persists for narrow packets.

The question now arises as to the lifetime of the multiple-peak structure. Does it eventually die out and the peaks merge? The answer to this question lies in the behaviour of the wavefunction inside the well. We will show below that the scattering proceeds through a metastable, quasi-bound, state inside the well. This state does not decay exponentially, but polynomially in time. Differing from the transient behaviour such as that of diffraction in time [9][1], for which oscillations are set up by a shutter that is suddenly opened, the peak structure persists for very long times. Thousands of times longer than the transit time of the packet through the interaction region. Instead of diffraction in time, we are witnessing a diffraction in space and time. From the numerical calculations, it appears that as far as we can observe the long-term behaviour is still multiple peaked[2].

We now proceed to review the results of the one-dimensional case and add some further results. The next section will be devoted to the two-dimensional case.

In [1] we used a minimal uncertainty wavepacket travelling from the left with an average speed v, initial location x_0, mass m, wavenumber $q = mv$ and width Δ,

$$\psi = C \exp\left(\mathrm{i}q(x - x_0) - \frac{(x - x_0)^2}{4\Delta^2}\right). \tag{1}$$

The attractive well was located around the origin, with depth V_0 and width parameter w. We used a Gaussian potential, but the results are not specific to this type of interaction,

$$V(x) = -V_0 \exp\left(-\frac{x^2}{w^2}\right). \tag{2}$$

The packet above contains only positive energy components and is therefore orthogonal to any bound state inside the well. Any such superposition will be hindered by factors of the form $\mathrm{e}^{-\kappa|x_0|}$, where $\kappa = \sqrt{2m|E_B|}$, with $|E_B|$ being the binding energy of the bound state. For initial locations x_0 far away from the well, this superposition vanishes. However, the initial packet is not orthogonal to metastable states or quasi-bound states at positive energies.

We solved the Schrödinger equation for the scattering event in coordinate space taking care of unitarity. We used the method of Goldberg *et al* [11], that proved to be extremely robust and conserves the normalization of the wavefunction, with an error of less than 0.01%, even after hundreds of thousands of time step iterations. We also verified that the solutions actually solve the equation with extreme accuracy by explicit substitution.

Figure 1 shows a series of pictures of the evolution of a narrow wavepacket. The impinging packet has a width of $\Delta = 0.5$, a momentum $q = 1$ and the well width is $w = 1$. We used a large mass $m = 20$ in order to prevent the packet from spreading too fast and to be on the safe side regarding relativistic effects [2].

The figure shows how the multiple-peak structure is produced early on. After $t = 200$, the reflected wave train surpasses the incoming wave and proceeds to propagate independently

[1] There has been a flurry of renewed interest in the subject in recent years (see, for example, [10]).

[2] This aspect will be addressed in a future work.

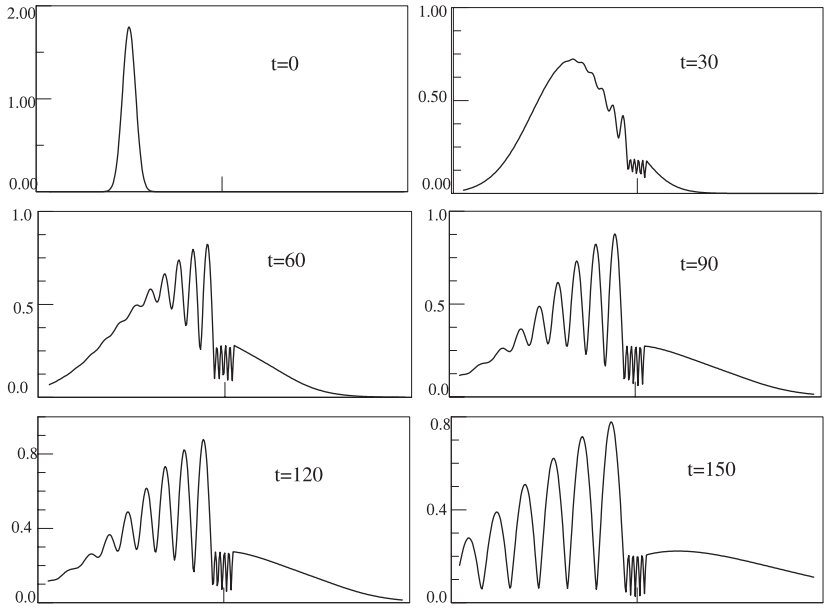

Figure 1. $|\Psi|$ as a function distance x for an initial wavepacket of width $\Delta = 0.5$ starting at $x_0 = -10$ impinging upon a well of width parameter $w = 1$ and depth $V_0 = 1$ at different times, the initial average momentum of the packet is $q = 1$.

of it. The effect persists for extremely long times. Figure 2 depicts the scattered waves after $t = 5000$, a time long enough for the waves to scatter at a large distance (recall that the well width is $w = 1$). A polychotomous (multiple-peak) wave recedes from the well. For low velocities, corresponding to average packet energies of less than half the well depth, several peaks in the reflected wave show up. Simple inspection reveals that the distance between the peaks is constant. The wave train propagates with an amplitude of the form

$$C(x) \approx \mathrm{e}^{-\lambda|x|} \sin^2(kx). \tag{3}$$

The exponential drop is characteristic of a virtual-state solution inside the well. The parameters λ and k, are independent of the initial velocity, but depend on time. The wave spreads and its amplitude diminishes, as expected. We corroborated that the polychotomous behaviour continues for as long time as we could check numerically.

Figure 3 shows the sequence of events for a wide packet.

The multiple peaks disappear completely for packets which are wider than the well. The long-time behaviour of the same case is depicted in figure 4. An approximate expression for the multiple-peak reflected packet average speed was found to be, $v = k(t_{formation})/m$, where k represents the wavenumber outside the well at the time it starts emerging from it after a long period of multiple reflections. This speed was found to be independent of the initial packet speed. The memory of the initial packet is deleted.

We investigated other types of potentials, such as a Lorentzian, a square well, etc, and found the same phenomena described here. Moreover, the effect is independent of the shape of the packet as long as it is narrower than the well width. We used square packets, Lorentzian packets, exponential packets, etc, with analogous results.

In order to find analytical support, we resorted to a square packet

$$\psi(x) = \mathrm{e}^{\mathrm{i}q(x-x_0)}\Theta(d - |x - x_0|) \tag{4}$$

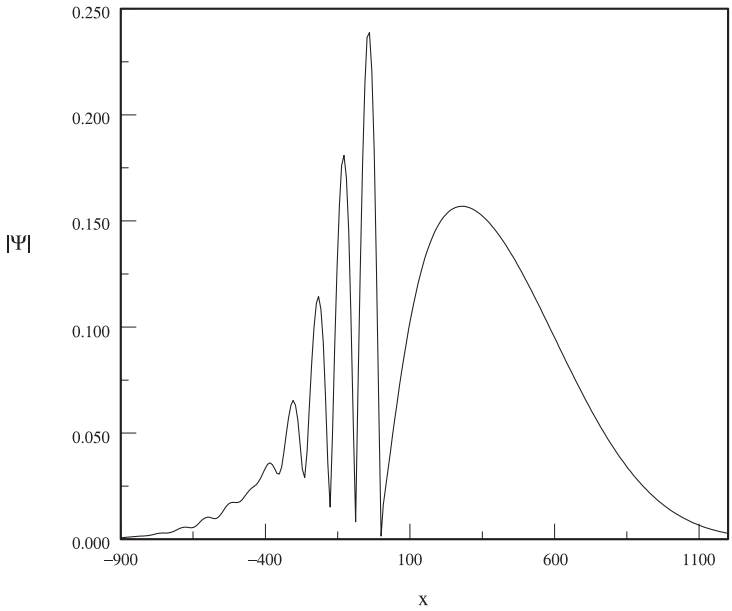

Figure 2. $|\Psi|$ as a function of distance x for an initial wavepacket of width $\Delta = 0.5$ starting at $x_0 = -10$ impinging upon a well of width parameter $w = 1$ and depth $V_0 = 1$ after $t = 5000$, the initial average momentum of the packet is $q = 1$.

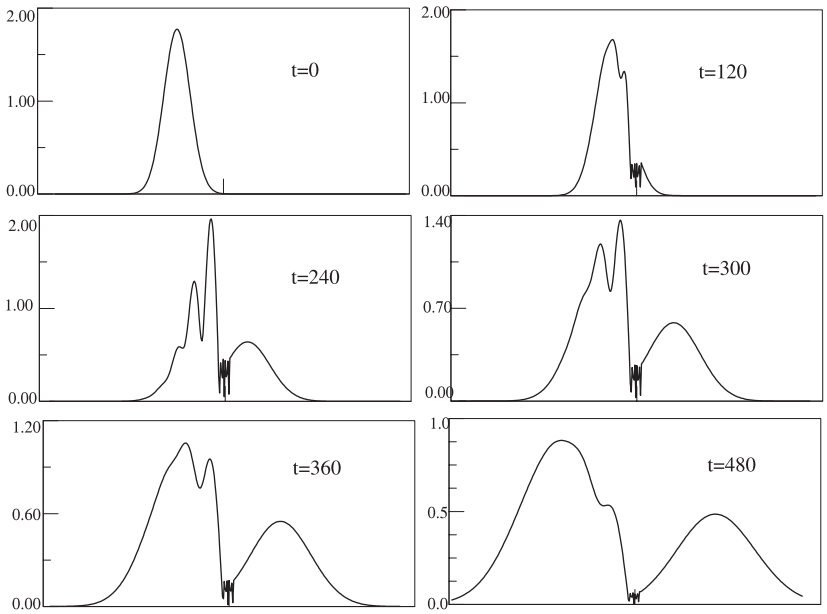

Figure 3. $|\Psi|$ as a function of distance x for an initial wavepacket of width $\Delta = 2$. Starting at $x_0 = -10$, impinging upon a well of width parameter $w = 0.5$ and depth $V_0 = 1$ at various times, the initial average momentum of the packet is $q = 1$.

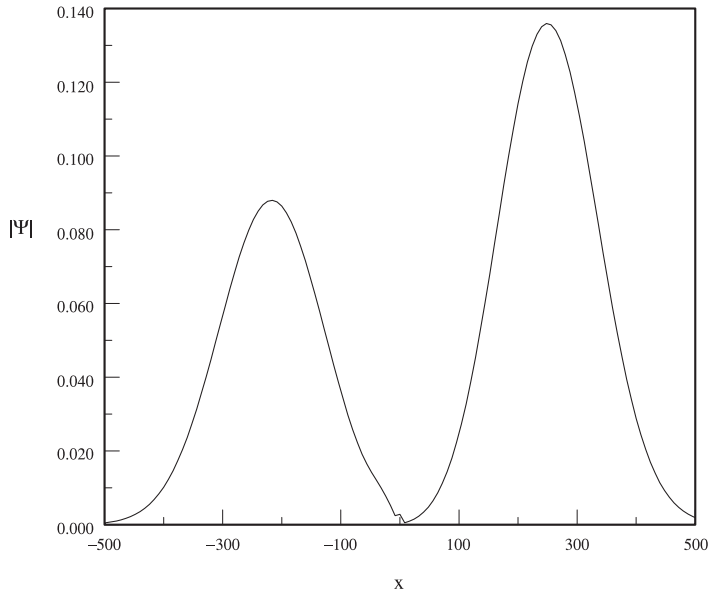

Figure 4. $|\Psi|$ as a function of distance x for an initial wavepacket of width $\Delta = 2$ starting at $x_0 = -10$, impinging upon a well of width parameter $w = 0.5$ and depth $V_0 = 1$ after $t = 5000$, the initial average momentum of the packet is $q = 1$.

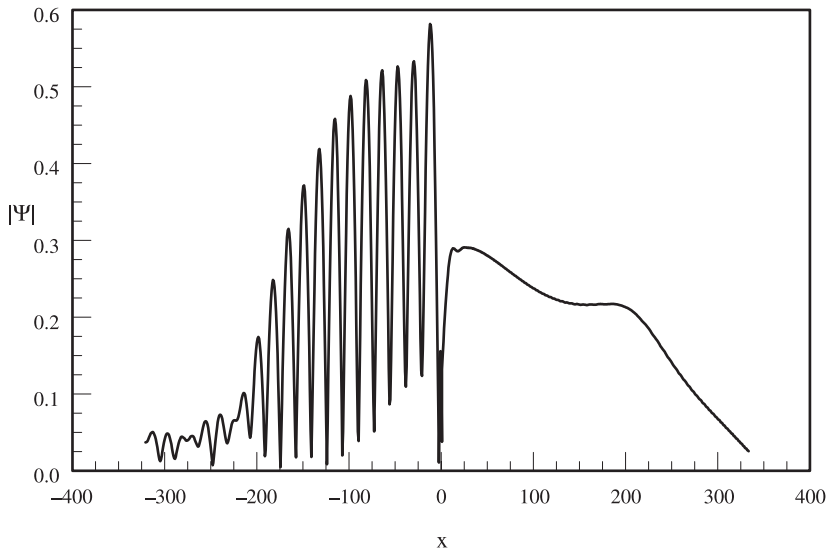

Figure 5. Theoretical calculation for a square initial packet scattering off a square well for $t = 1000$.

where d is half the width of the packet, x_0 is the initial position and q is the wavenumber. It impinges on a square well located at the origin, whose width is $2a$ and depth V_0

$$V(x) = -V_0\Theta(a - |x|). \tag{5}$$

This case is solvable using the techniques of [12]. The method is appropriate only for packets

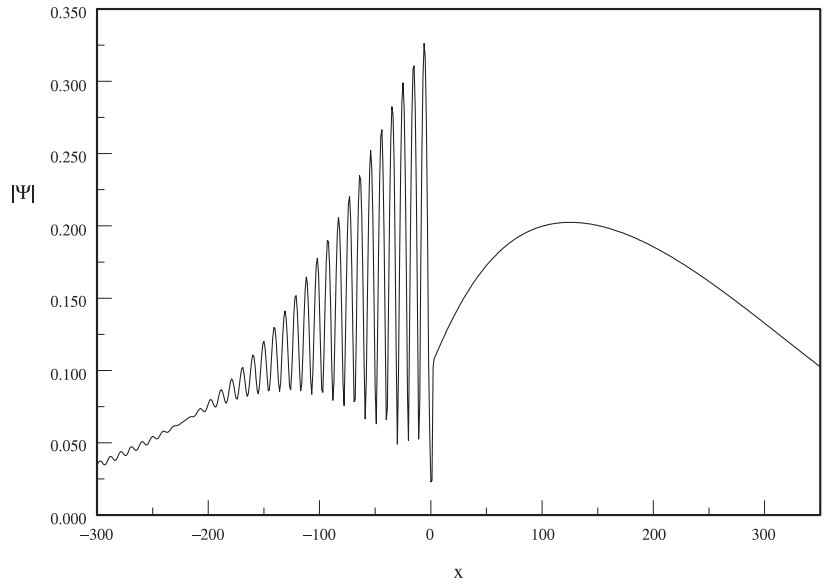

Figure 6. $|\Psi|$ as a function distance x for an initial wavepacket of width $\Delta = 0.5$ starting at $x_0 = -50$, impinging upon a well of width parameter $w = 1$ and depth $V_0 = 1$ after $t = 3000$, the initial average momentum of the packet is $q = 1$.

with sharp edges, that terminate at a certain point. It consists of integrating the Fourier amplitude of the wave using a contour in the complex momentum plane that avoids the poles of the scattering matrix corresponding to the bound states. For each momentum, one uses the appropriate stationary scattering state for the square well. The integral reads

$$\psi(x, t) = \int_C \phi(x, p) a(p, q)\, \mathrm{d}p \tag{6}$$

where C is a contour that goes from $-\infty$ to $+\infty$ and circumvents the poles that are on the imaginary axis for $P < \mathrm{i}\sqrt{2mV_0}$ by closing it above them. $\Phi(x, p)$ is the stationary solution to the square-well scattering problem for each p and $a(p, q)$ is the Fourier transform amplitude for the initial wavefunction with average momentum q. The results are depicted in figure 5. The initial wavepacket had average momentum $q = 1$, width $\Delta = 0.5$, and the square well parameters were $V_0 = 1, a = 1$. The reflected wave shows exactly the same polychotomous behaviour as the numerical simulations. In particular, numerical calculations with a square packet and a square well match the analytical results almost exactly.

The polychotomous effect is general, even the packet amplitude becomes unimportant. The very existence of the effect does not depend on the initial position of the packet, as mentioned in passing in [1]. Figure 6 shows one such case for the same parameters as those of figure 1, but an initial location of $x_0 = -50$. The number of peaks has increased and the distance between them has shrunk. There appears a smooth background under the multiple peaks. The well reacts to the presence of the packet from far away. So, even if the packet is narrower only far away from the well, the polychotomous structure persists, despite the normal spreading that must occur until the centre of the packet reaches the well, which, in the depicted case, would amount to many times the original width.

It was claimed above that the multiple-peak effect was due to the interference between incoming and reflected waves. A sign of its persistence may be found in the behaviour of the

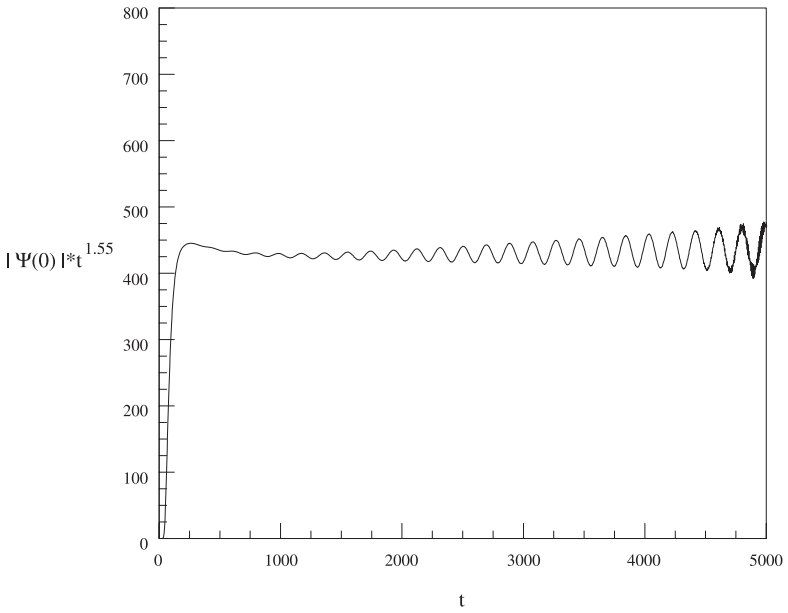

Figure 7. $|\psi(0)|$ as a function of time for the scattering depicted in figure 1.

wave inside the well. The amplitude of the wavefunction at the origin as a function of time provides us with a suitable index to characterize it. The long-time behaviour of the decay of this amplitude is polynomial. Trial and error lead us to a fit with a polynomial of the form $|\psi(0)| = C/t^{1.55}$, with c, a constant. Figure 7 shows this time dependence for the case of a narrow packet.

In the conventional manner of defining the lifetime for exponential decay, such as is done for virtual states, the metastable state inside the well would have an infinite lifetime. Although this is not a proof at all, the numerical results strongly suggest that, if not infinite, the lifetime of the metastable state is extremely large. Instead of being a mere transient effect, that disappears after a time comparable to the transit time of the packet through the well, as for other transients, such as the diffraction in time process [9, 10], it looks as if the diffraction pattern persists. The metastable state inside the well is, in a way, a decaying trapped state.

3. Two-dimensional wavepacket scattering from an attractive well

The results of the previous section call for a more realistic calculation. As a step towards a full three-dimensional calculation, we proceed here to describe the results of the two-dimensional case.

Consider two-dimensional scattering off a potential well as described by the time-dependent Schrödinger equation

$$\frac{-1}{2m}\left(\frac{\partial^2}{\partial r^2}+\frac{\partial}{r\partial r}+\frac{\partial^2}{r^2\partial\phi^2}\right)\Phi + V(r)\Phi = \mathrm{i}\frac{\partial\Phi}{\partial t}. \tag{7}$$

where ϕ is the polar angle and r is the radial coordinate. Expanding in partial waves,

$$\Phi(t, r, \phi) = \sum_{l=0}^{l_{max}} \mathrm{e}^{\mathrm{i}l\phi}\phi_l(r, t) \tag{8}$$

we obtain decoupled partial wave equations (the potential is assumed independent of ϕ),

$$\frac{-1}{2m}\left(\frac{\partial^2}{\partial r^2}+\frac{\partial}{r\partial r}-\frac{l^2}{r^2}\right)\phi_l+V(r)\phi_l=\mathrm{i}\frac{\partial\phi_l}{\partial t}. \tag{9}$$

A further simplification is achieved by the substitution $\Phi_l = \tilde{\Psi}_l/\sqrt{r}$. The potential acquires an extra term and the first derivative cancels out. Henceforth we work with the wavefunction $\Psi = \Phi\sqrt{r}$. This substitution also allows for a simple numerical treatment. For each partial wave we apply the method used in the one-dimensional case [11].

We start the scattering event of a minimal uncertainty wavepacket

$$\Psi_0 = C\sqrt{r}\exp\left(\mathrm{i}q(x-x_0)-\frac{(x-x_0)^2+(y-y_0)^2}{4\Delta^2}\right) \tag{10}$$

at a distance large enough to be outside the range of the potential,

$$V(r) = -A\exp\left(-\frac{r^2}{w^2}\right) \tag{11}$$

for which we again use a Gaussian.

We present our results for different impact parameters y_0, for a packet travelling initially along the negative x-axis towards the well, with average speed $v = q/m$ as a function of angle and distance from the location of the potential.

Figures 8–10 show the scattered waves at angles of 180°, 90° and 0°, respectively, for initial momenta $q = 1, 2, 3$ in inverse distance units. The initial centre of the packet is at $x_0 = -10$, $y_0 = 0$. The parameters of the well are $w = 2$, $V_0 = 1$, the width of the initial packet $\Delta = 0.5$. Throughout the calculation we limited the number of partial waves to $l_{max} = 50$. The accuracy in the expansion obtained with this limit, was found to be better than

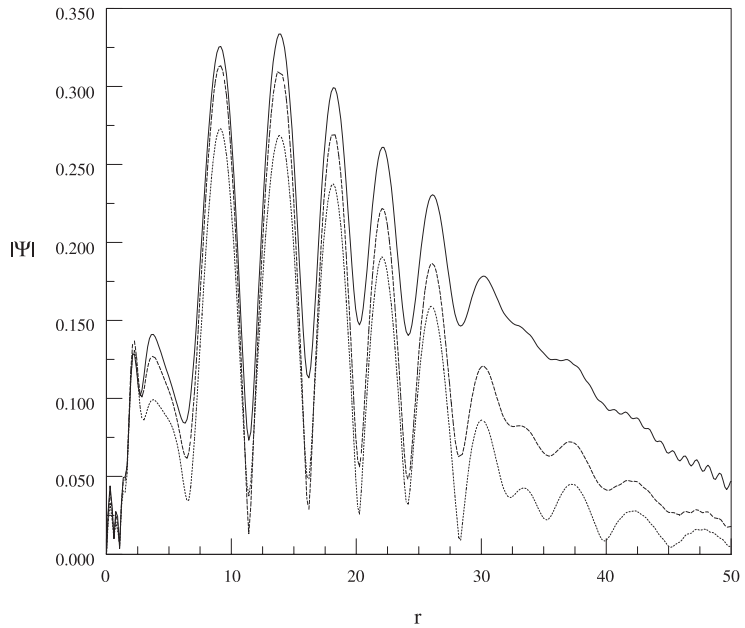

Figure 8. $|\Psi|$ at an angle of 180°, as a function of r at $t = 300$. Wavepacket width $\Delta = 0.5$, $x_0 = -10$, $y_0 = 0$. Well width, $w = 2$ depth $V_0 = 1$. Average momenta of the packet were $q = 0.5$ (full curve), $q = 1$ (broken curve), $q = 1.5$ (dotted curve).

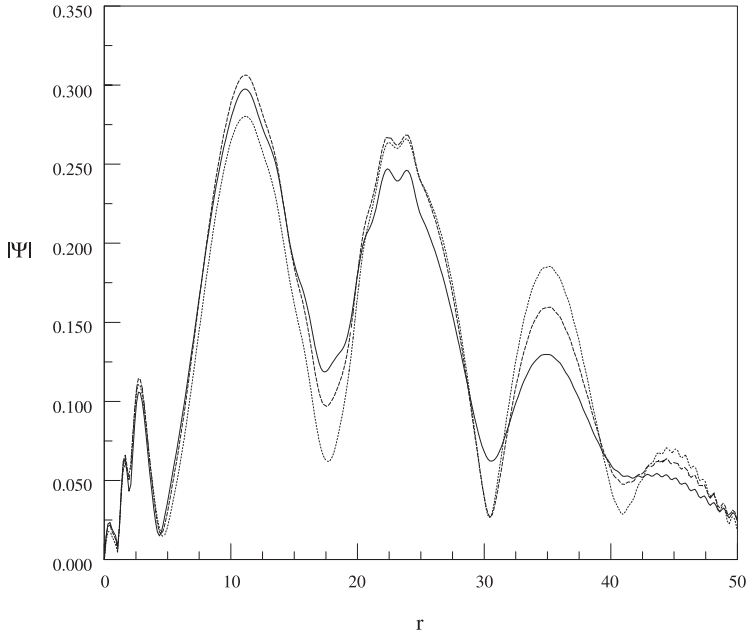

Figure 9. $|\Psi|$ at an angle of 90°, as a function of r at $t = 300$. Wavepacket width $\Delta = 0.5$, $x_0 = -10$, $y_0 = 0$. Well width, $w = 2$ depth $V_0 = 1$. Average momenta of the packet were $q = 0.5$ (full curve), $q = 1$ (broken curve), $q = 1.5$ (dotted curve).

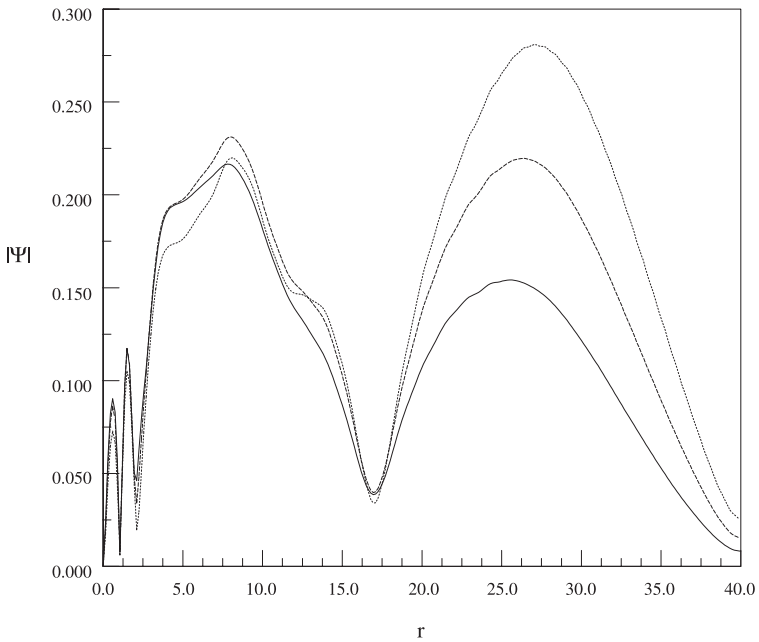

Figure 10. $|\Psi|$ at an angle of 0°, as a function of r at $t = 300$. Wavepacket width $\Delta = 0.5$, $x_0 = -10$, $y_0 = 0$. Well width, $w = 2$ depth $V_0 = 1$. Average momenta of the packet were $q = 0.5$ (full curve), $q = 1$ (broken curve), $q = 1.5$ (dotted curve).

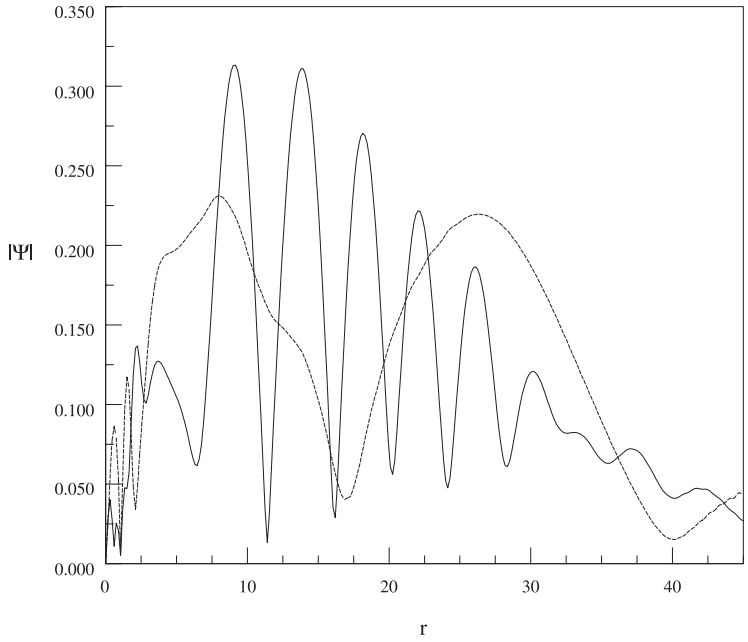

Figure 11. $|\Psi|$s at 180° (full curve), and 0° (broken curve) for a packet with $q = 1$ and zero impact parameter at $t = 300$. Well parameters remain as in figure 7.

1%. For large impact parameters we increased the number of partial waves up to $l_{max} = 70$. The wavefunctions are normalized to 2π.

The figures show clearly that the same phenomenon found in the one-dimensional case emerges in two dimensions. Even at small angles the effect persists, although the multiple-peak structure is cleaner in the backward direction. Figure 11 shows the comparison between backward and forward scattering for impact parameter $y_0 = 0$. Large-angle scattering shows up as an extremely important element.

Figures 12 and 13 show the behaviour of the scattered wave at large and small angles for increasing impact parameter.

At backward angles, the impact parameter influences the shape of the pattern very little. The memory of the initial information concerning impact parameter—and even momentum, for moderate momenta as compared with the inverse of the well width—is erased.

We can visualize the existence of a quasi-bound state inside the well by selecting the region around the origin and plotting real and imaginary parts of the wavefunction. Figures 14 and 15 show these waves for masses $m = 20$ and 5,respectively, for backward angles. Here we depicted Φ instead of Ψ. As for the one-dimensional case, we see a sinusoidal behaviour. For $m = 20$ it is seen that the well width accommodates approximately two wavelengths, while for $m = 5$ one wavelength fits in. (Recall that the well does not have a sharp edge.) From the figures we can read off the value of the wavenumber inside the well, namely $k' = \sqrt{k^2 + 2m|V_0|}$ to be $k' = \frac{2\pi n}{2w}$. For $m = 20$ we find $n = 2$, and for $m = 5$ we find $n = 1$. Inserting the values of the mass and the depth of the potential V_0, we obtain $k \approx 0$.

The two-dimensional case resembles remarkably the one-dimensional scattering, for packets that are initially narrower than the well. This is also true for the scattering of wide

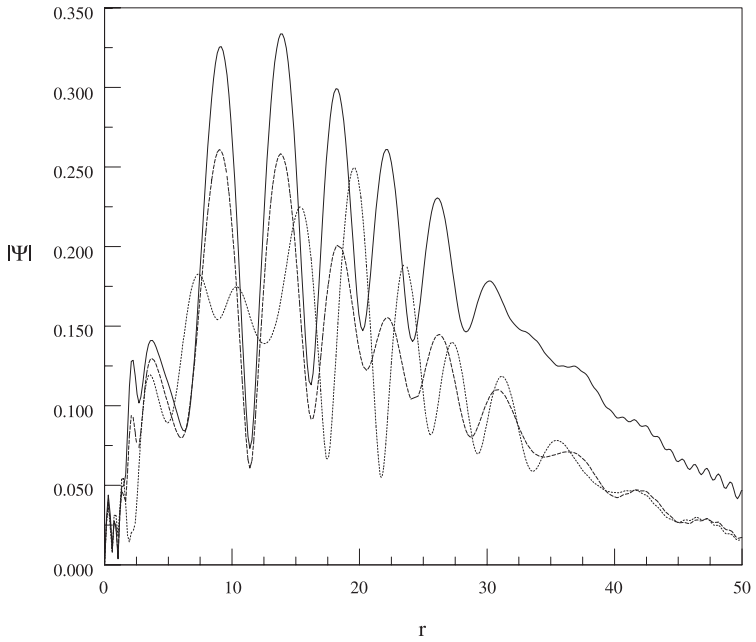

Figure 12. $|\Psi|$s at 180° for impact parameter $y_0 = 0$, full curve, $y_0 = 1.5$, broken curve, and $y_0 = 3$, dotted curve at $t = 300$. Well and packet parameters as in figure 7.

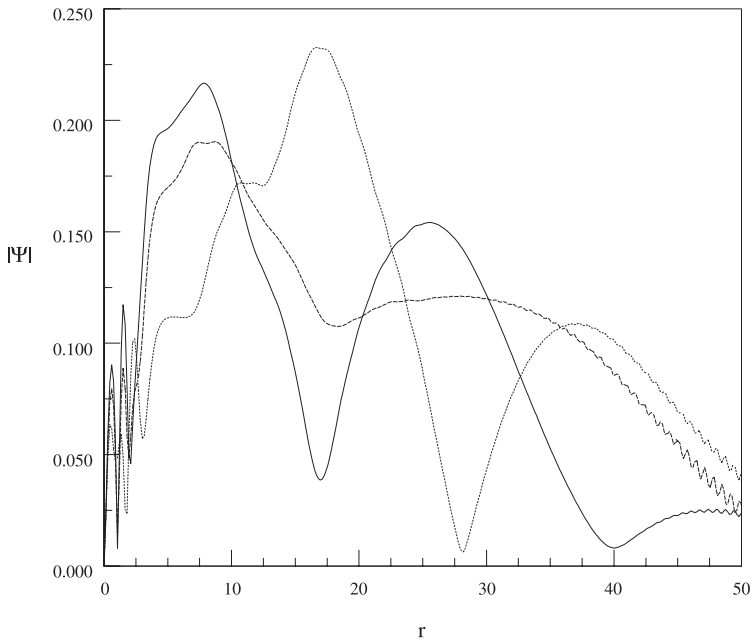

Figure 13. $|\Psi|$ at 0° for impact parameter $y_0 = 0$, full curve, $y_0 = 1.5$, broken curve, and $y_0 = 3$, dotted curve at $t = 300$. Well and packet parameters as in figure 8.

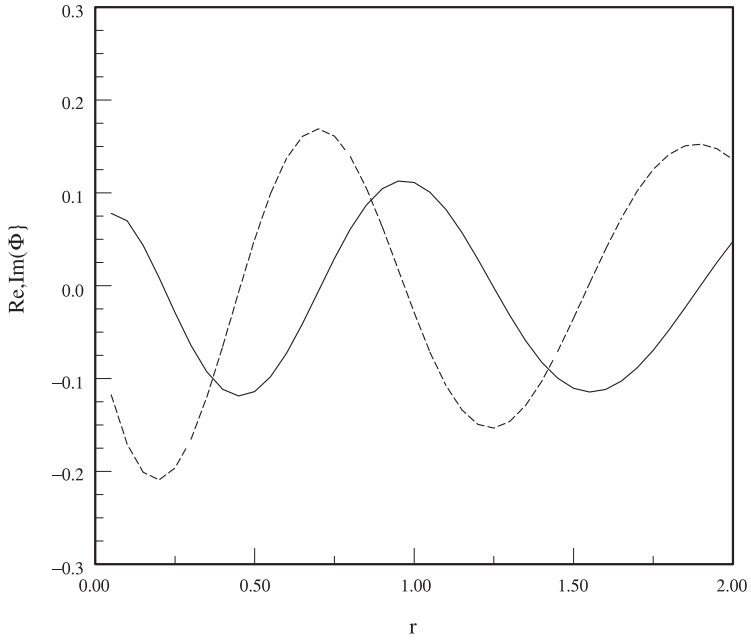

Figure 14. Real (full curve) and imaginary (broken curve) part of Φ at 180° for impact parameter $y_0 = 0$, momentum $q = 1$, mass $m = 20$, in a region inside the well at $t = 150$.

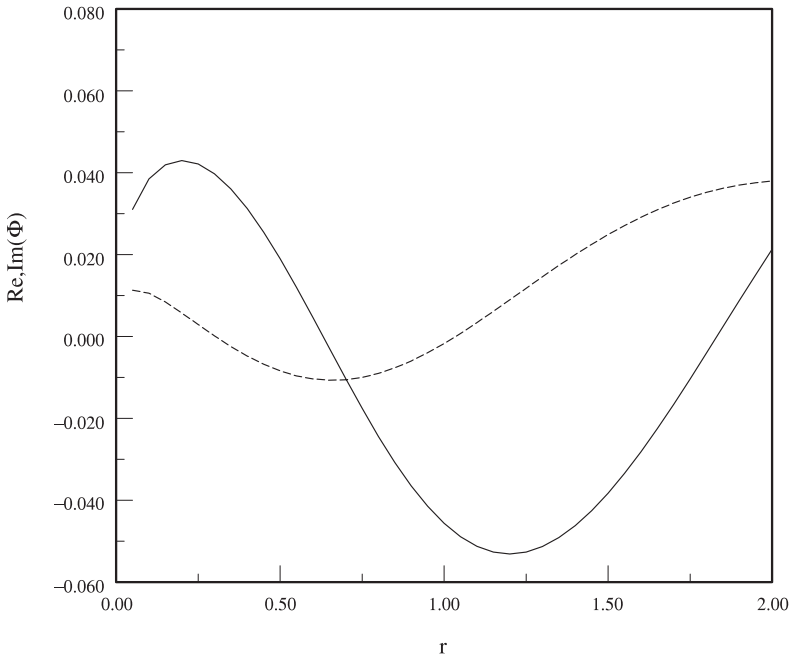

Figure 15. Real (full curve) and Imaginary (broken curve) part of Φ at 180° for impact parameter $y_0 = 0$, momentum $q = 1$, mass $m = 5$, in a region inside the well at $t = 150$.

packets. Figures 16–18 show that all the polychotomous wave trains disappear when the initial packet is wider than the well. The multiple peaks are now absent. Forward and backward scatterings look now quite similar.

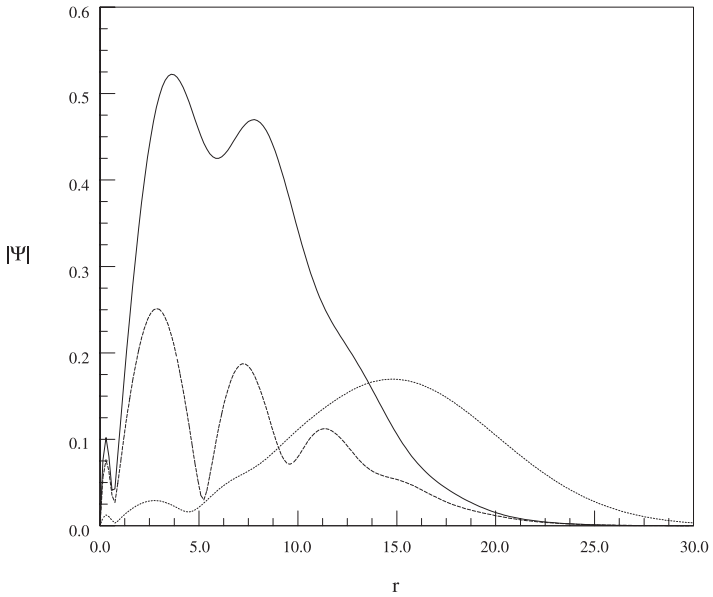

Figure 16. $|\Psi|$ at an angle of 180°, as a function of r. Wavepacket width $\Delta = 2$, $x_0 = -10$, $y_0 = 0$. Well width, $w = 0.5$ depth $V_0 = 1$. Average momenta of the packet were $q = 0.5$ (full curve), $q = 1$ (broken curve), $q = 1.5$ (dotted curve) at $t = 300$.

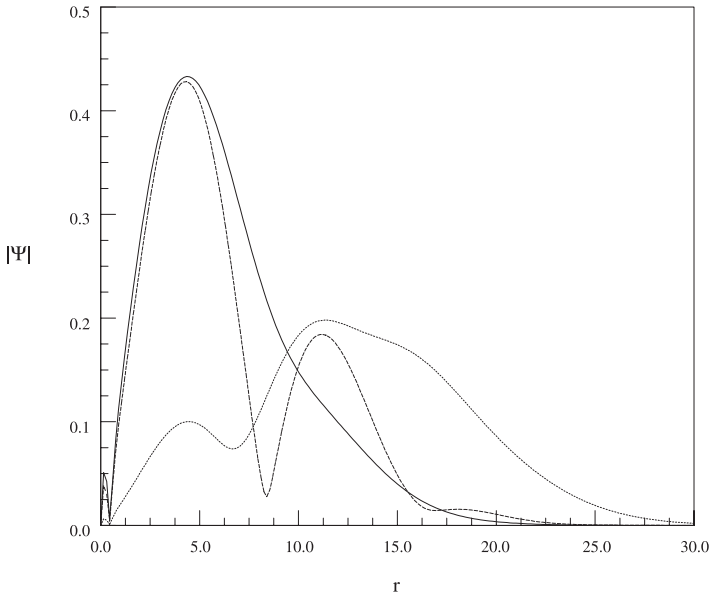

Figure 17. $|\Psi|$ at an angle of 90°, as a function of r. Wavepacket width $\Delta = 2$, $x_0 = -10$, $y_0 = 0$. Well width, $w = 0.5$ depth $V_) = 1$. Average momenta of the packet were $q = 0.5$ (full curve), $q = 1$ (broken curve), $q = 1.5$ (dotted curve) at $t = 300$.

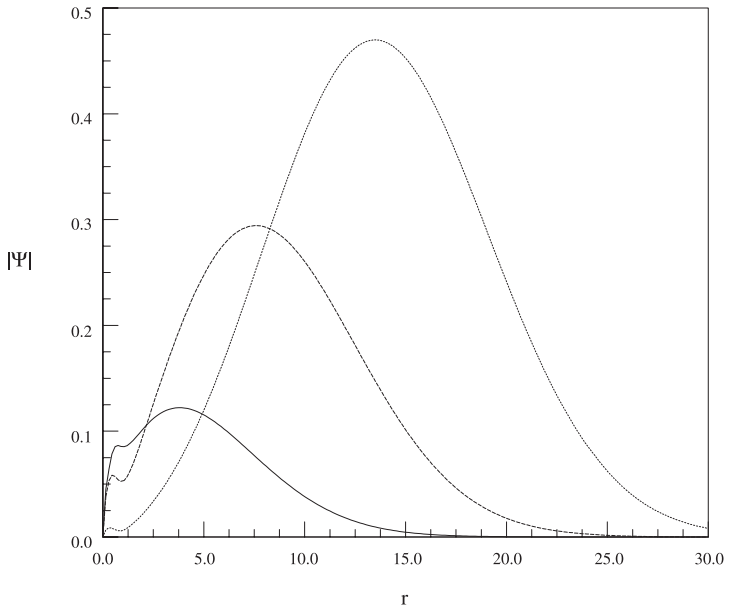

Figure 18. $|\Psi|$ at an angle of 0°, as a function of r. Wavepacket width $\Delta = 2$, $x_0 = -10$, $y_0 = 0$. Well width, $w = 0.5$ depth $V_0 = 1$. Average momenta of the packet were $q = 0.5$ (full curve), $q = 1$ (broken curve), $q = 1.5$ (dotted curve) at $t = 300$.

The effect depends on the existence of a quasi-bound state inside the well. Shallow potentials cannot sustain the metastable states. Therefore, the polychotomous behaviour should gradually disappear when the depth of the well is diminished. Figure 19 shows one such case for a well amplitude of $A = 0.03$

4. Suggested experiments

We have found that the polychotomous coherent effect of [1], persists in two dimensions and presumably this will be true in a full three-dimensional calculation. Experimental work may take advantage of these findings and design set-ups to research the phenomena described here. We mentioned in section 1 the possibility of using cavity experiments with atomic beams, the assessment of the feasibility of such experiments is, however, beyond the knowledge of the author, although it appears to be a tangible option. Experiments in optics, sound propagation, microwaves, might also be appropriate in order to find the polychotomous behaviour. Another alternative that seems viable, consists in an experiment related to those known under the title of *ALAS* [6].

ALAS denotes anomalous large-angle scattering. It occurs for α scattering on certain closed shell nuclei for incident energies below 100 MeV. The backward scattering is so pronounced that can exceed the Rutherford cross section by several orders of magnitude. Although many explanations based on optical models have been provided over the years for this process, it remains rather obscure. A possible interpretation based on the present results would be that, the α particle is a finite-extent system of dimensions smaller than the nuclear well. Considered as a wavepacket it could form a metastable state inside the well in a similar manner to the packets dealt with presently. The large backward scattering is then a reflection of the behaviour found here for a finite size packet. A clear imprint of the effect would, however,

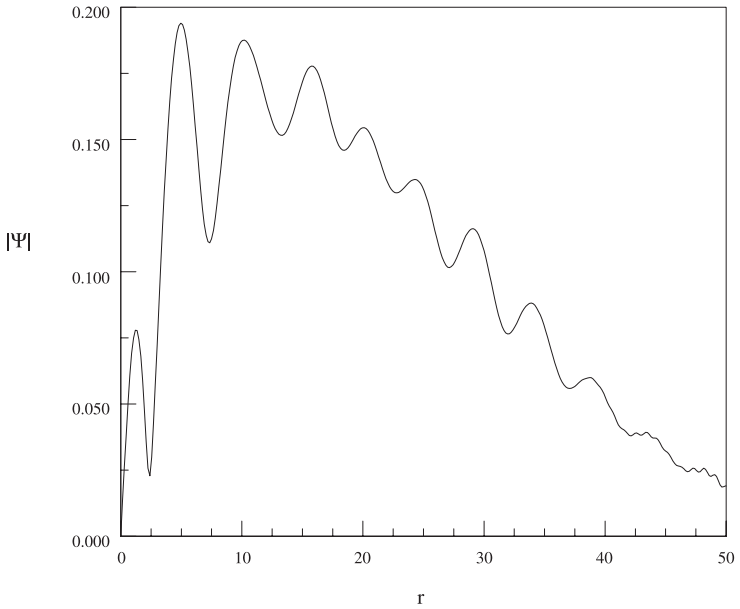

Figure 19. $|\Psi|$ for a scattering angle of 180°, packet width $\Delta = 0.5$ starting at $x_0 = -10$, impinging upon a well of width parameter $w = 2$ and depth $V_0 = 0.03$ at $t = 300$, the initial average momentum of the packet is $q = 1$, with a mass of $m = 20$.

require the detection of the α particles as a function of time in order to observe the oscillatory amplitudes that dominate at large scattering angles. Data acquisition in nuclear (and other) experiments generally averages over time variations, except for coincidence experiments. The multiple-peak behaviour demands a continuous time-dependent recording of the alpha particles, triggered by the bunches emitted from the accelerating machine. If experimental support is indeed gathered, then the effect can be turned around in order to become a research tool, due to its dependence on the geometrical and dynamical parameters of both projectiles and target. A firm theoretical connection to the *ALAS* effect, requires, eventually, a much more laborious theoretical and numerical work than the one carried out here. Efforts in that direction are currently underway.

Acknowledgments

This work was supported in part by the Department of Energy under grant DE-FG03-93ER40773 and by the National Science Foundation under grant PHY-9413872, while the author was on sabbatical at the cyclotron institute of the Texas A&M University. It is a pleasure to thank Professor Youssuf El Masri of the UCL, University of Lovain-la-Neuve, Belgium for the information concerning the ALAS effect.

References

[1] Kälbermann G 1999 *Phys. Rev.* A **60** 2573
[2] Merzbacher E 1970 *Quantum Mechanics* (New York: Wiley)
[3] Yeazell J and Uzer T (ed) 2000 *The Physics and Chemistry of Wave Packets* (New York: Wiley)
[4] Goldberger M L and Watson K M 1964 *Collision Theory* (New York: Wiley)

[5] Tannor D J 2001 *Introduction to Quantum Mechanics: a Time Dependent Perspective* at press
[6] Brau F, Michel F and Reidemeister G 1998 *Phys. Rev.* C **57** 1390 and references therein
[7] Grobe R and Fedorov M V 1992 *Phys. Rev. Lett.* **68** 2592
[8] Schiff L 1968 *Quantum Mechanics* 3rd edn (New York: McGraw-Hill) pp 108–9
[9] Moshinsky M 1952 *Phys. Rev.* **88** 625
[10] Xiao M 1999 *Phys. Rev.* E **60** 6226
[11] Goldberg A, Schey H M and Schwartz J L 1967 *Am. J. Phys.* **35** 177
[12] Weber T L and Hammer C L 1977 *J. Math. Phys.* **18** 1562
Hammer C L and Weber T L 1967 *J. Math. Phys.* **8** 494
Hammer C L, Weber T L and Zidell V S 1977 *Am. J. Phys.* **45** 933
Hammer C L, Weber T L and Zidell V S 1982 *Am. J. Phys.* **50** 839